Adaptive margins for online adaptive radiotherapy

Bijl, E. van der; Remeijer, P.; Sonke, J.J.; Heide, U.A. van der; Janssen, T.

IOP Publishing Phys. Med. Biol. 67 (2022) 195016 https://doi.org/10.1088/1361-6560/ac9175

Physics in Medicine & Biology

IPEM Institute of Physics and Engineering in Medicine

OPEN ACCESS

RECEIVED
8 May 2022

REVISED
25 August 2022

ACCEPTED FOR PUBLICATION
12 September 2022

PUBLISHED
30 September 2022

PAPER

Adaptive margins for online adaptive radiotherapy

Erik van der Bijl[1], **Peter Remeijer**[2], **Jan-Jakob Sonke**[2], **Uulke A van der Heide**[2] **and Tomas Janssen**[2]

[1] Department of Radiation Oncology, Radboud University Medical Center, Nijmegen, The Netherlands
[2] Department of Radiation Oncology, The Netherlands Cancer Institute, Amsterdam, The Netherlands

E-mail: erik.vanderbijl@radboudumc.nl

Keywords: adaptive radiotherapy, image-guided radiotherapy, margins

Supplementary material for this article is available online

Abstract

Objective. In online adaptive radiotherapy a new plan is generated every fraction based on the organ and clinical target volume (CTV) delineations of that fraction. This allows for a planning target volume margin that does not need to be constant over the whole course of treatment, as is the case in conventional radiotherapy. This work aims to introduce an approach to update the margins each fraction based on the per-patient treatment history and explore the potential benefits of such adaptive margins. *Approach.* We introduce a novel methodology to implement adaptive margins, isotropic and anisotropic, during a treatment course based on the accumulated dose to the CTV. We then simulate treatment histories for treatments delivered in up to 20 fractions using various choices for the standard deviations of the systematic and random errors and homogeneous and inhomogeneous dose distributions. The treatment-averaged adaptive margin was compared to standard constant margins. The change in the minimum dose delivered to the CTV was compared on a patient and a population level. All simulations were performed within the van Herk approach and its known limitations. *Main results.* The population mean treatment-averaged margins are down to 70% and 55% of the corresponding necessary constant margins for the isotropic and anisotropic approach. The reduction increases with longer fractionation schemes and an inhomogeneous target dose distribution. Most of the benefit can be attributed to the elimination of the effective systematic error over the course of treatment. Interpatient differences in treatment-averaged margins were largest for the isotropic margins. For the 10% of patients that would receive a lower than prescribed dose to the CTV this minimum dose to the CTV is increased using the adaptive margin approaches. *Significance.* Adaptive margins can allow to reduce margins in most patients without compromising patients with greater than average target motion.

1. Introduction

Modern platforms that allow for image-guided online adaptive radiotherapy, using magnetic resonance imaging or cone beam CT are rapidly expanding their base of installations (Mutic and Dempsey 2014, Acharya *et al* 2016, Raaymakers *et al* 2017, Winkel *et al* 2019). These systems combine improved image quality with the possibility to daily adapt the delineations and re-optimize the plan. Online treatment plan adaptation and re-optimization are expected to become common practice in radiotherapy in the coming years (Sibolt *et al* 2021).

By daily updating the treatment plan, interfraction uncertainty will decrease and the main positioning uncertainty left is intrafraction anatomical changes and target motion. Moreover, due to daily delineation and replanning, systematic errors in those steps become more random in nature. Therefore, planning target volume (PTV) margins can be reduced for online plan adaptation. The magnitude of these margin reductions is still being explored for most treatment sites (de Muinck Keizer *et al* 2020).

The well-known and widely used van Herk margin recipe (Van Herk 2004, Van Herk *et al* 2000) is based on the premise that a margin is sufficient when the dose delivered to the clinical target volume (CTV) reaches a

fraction q of the prescribed dose for p percent of the population, with common choices $q = 0.95$ and $p = 90\%$. Since this means that the margin is determined by the 10% patients with the largest errors, margins for individual patients can be improved by including individualized information compared to population based estimates. Patient-specific motion patterns for example have been used for individualised margins in conventional radiotherapy approaches such as libraries of plans (Collins and Leech 2018) and individual margins to account for respiratory motion (Peulen *et al* 2014). In these approaches, the patient-specific reproducibility of the movement of the bladder (De Ahmad *et al* 2013, Jong *et al* 2020) or respiratory pattern are exploited to reduce margins.

Margin recipes are based on the expected delivered dose, but could potentially be improved by taking into account the actual delivered dose of previous fractions, and in this way account for anatomical change during the course of treatment. A tempting thought is to reduce the PTV margins if the CTV motion was small in the previous fractions. In this way, patients that happen to have a smaller target motion than the population average will end up with a smaller overall treatment margin. The opposite logic can applied as well: if motion is larger than the margin tolerates, the PTV margin can be increased to ensure CTV coverage. Since adaptive plans are optimized every fraction, it is relatively straightforward to implement such an adaptive PTV margin in an online adaptive workflow. Alternative approaches were the dose is increased locally to account for an underdosage in previous fractions are explicitly not considered, In this work we explicitly keep the prescribed dose per fraction constant and only adjust the margins.

The aim of this study is to investigate and quantify the possible benefit of daily margin adaptation in online adaptive radiotherapy for individual patients. To this end, we simulate radiation treatments, with similar assumptions as in the van Herk approach: spherical, rigid tumours, treated with an isotropic, conformal dose distribution, for a finite number of fractions (De Boer and Heijmen 2001, Gordon and Siebers 2007, Herschtal *et al* 2012). We consider adaptive margins that are updated each fraction. Where the margin for the current fraction is determined from the accumulated dose over the previous fractions and the number of fractions that remain to be given. In order to keep the problem tractable, understandable and in line with existing literature we perform our simulations within the idealised situation of the van Herk recipe and do not account explicitly for the additional uncertainties caused by the dose accumulation.

First, we introduce our methodology for obtaining isotropic adaptive margins based on the accumulated dose over the already given fractions, and subsequently generalize this to anisotropic adaptive margins. In order to apply and evaluate these methods we consider the adaptive margin recipe within the classical margin framework and then describe how treatment histories were simulated for various choices of systematic and random errors. Besides these parameters, we consider two different cases, an homogeneously planned dose distribution and an inhomogeneous planned dose distribution to gauge the influence of dose inhomogeneity on the adaptive margin approaches. We continue with a comparison of the average margins over a course of treatment as given by the two adaptive margin approaches to the classical margins that are constant over the course of treatment. In order to make a fair comparison we compare the adaptive approaches, which by construction work for a finite number of fractions to the classical margin approach obtained for a finite number of fractions via simulations. We elaborate further on the motivation and clinical relevance of these assumptions and explored parameter values in the discussion.

2. Materials/methods

2.1. Model description

2.1.1. Adaptive margin recipe

The aim of the margin proposed here is, similar to the classical margin recipes (Van Bel *et al* 1996, Van Herk 2004, Herk *et al* 2000), that after N fractions of radiotherapy, the minimum dose to the CTV is at least q times the prescribed dose for p percent of the population. Commonly used choices are $q = 0.95$ and $p = 90\%$ for conventional radiotherapy with a homogeneous dose distribution in the target and $q = 0.80$ for inhomogeneous dose distributions as often applied in stereotactic radiotherapy (Peulen *et al* 2014). Within this work all dose will be normalized to the prescribed dose and we denote the target dose as q such that $q = 1.0$ means the CTV is covered by the prescribed dose.

The rationale for the adaptive margin recipe that we propose is the following. For simplicity we shall first describe the approach using an isotropic margin. We define the margin function $M(N, q, p)$ as the function that yields *constant* classical margin required for radiotherapy delivered in N fractions to administer the target dose q to the CTV, for p percent of the population.

The adaptive margin for fraction $n + 1$ depends on the accumulated minimum dose to the CTV after the previous n fractions, denoted as D_n. This accumulated minimum dose, as a fraction of the prescribed dose, is related to the dose per fraction $d_i(\vec{r})$ via

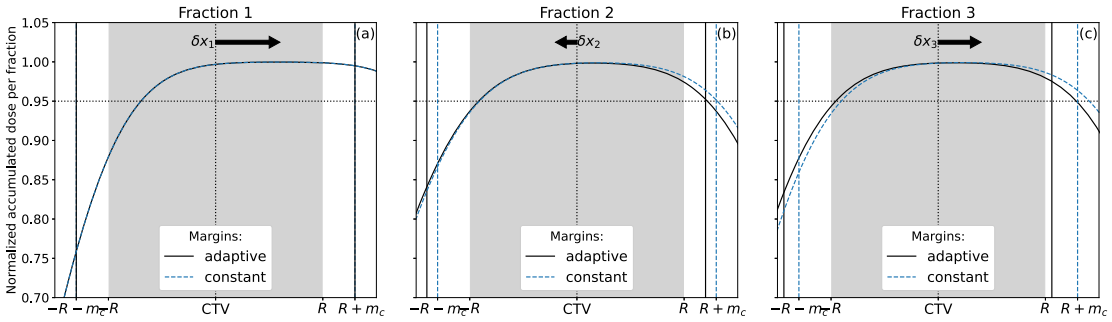

Figure 1. Illustration of the effect of the anisotropic adaptive margin (solid lines) recipe on the accumulated dose for three fraction radiotherapy in the one dimensional situation, compared to the classical constant margin approach (dashed lines). The normalized accumulated dose per fraction is plotted for these two methods. The vertical lines indicate the margins used each fraction, which are equal to the constant margins m_c. The first fraction (a), the anisotropic adaptive and constant margins are the same. A large displacement of $\delta x_1 = 2m_c$ to the right results in a higher than desired dose at the right and a lower than expected dose at the left end of the CTV (shaded area). The second fraction (b) is planned with the anisotropic adaptive margins adjusted according to the accumulated dose after the first fraction, thus increasing the margins on the left while reducing them on the right. The effect of the random displacement in fraction 2: $\delta x_2 = -0.8m_c$ to the left results in a small difference in the accumulated dose for to adaptive and classical constant margins. After the third fraction (c) and another shift $\delta x_3 = 1.2m_c$ to the right has occurred. The CTV is covered by the desired dose only in the adaptive anisotropic margins case while reducing the average margin used over the course of treatment.

$$D_n = \min_{\vec{r}\in \mathrm{CTV}} \sum_{i=1}^{n} d_i(\vec{r}), \tag{1}$$

where the minimum runs over all positions $\vec{r}$ within the CTV. The margin for fraction $n+1$ is obtained under the assumption that this margin will be used for the remainder of the treatment such that the dose q is reached in p percent of the population, given that the dose D_n is already delivered. In order to arrive at the desired dose q after N fractions we have to deliver a target dose q_n in the remaining N-n of the fractions, which is given by

$$q_n = \frac{N\,q - D_n}{N - n}, \tag{2}$$

The margin for fraction $n+1$ can then be obtained from the constant margin formula, via

$$m_{n+1}(N, q, p) = M(N - n, q_n, p). \tag{3}$$

Via the patient-specific accumulated dose a personalized adaptive margin is obtained from the population based margin function. Note that adaptive margin for the first fraction ($n = 0$ fractions delivered) is just $M(N, q, p)$, which equals the classical constant margin which we for clarity denote as m_c.

The more elaborate anisotropic approach follows from replacing the accumulated minimal dose D_n with $D_n(\vec{r})$, the accumulated dose at the edge of the CTV in the direction $\vec{r}$. $D_n(\vec{r})$ follows from equation (1) by omitting the min operation. As a consequence, both q_n and m_n become depended on these directions via equations (2), (3) upon replacement of $D_n \rightarrow D_n(\vec{r})$. This approach results in an anisotropic margin around the CTV. For details see the supplementary information (available online at stacks.iop.org/PMB/67/195016/mmedia), section 1.

Figure 1 illustrates how the margins are updated anisotropically throughout the course of treatment in a one dimensional example for three fractions for an individual treatment. In the example the anisotropic adaptive margins are on average smaller than the constant margins, and adjust themselves to the motions over the course of treatment, in supplementary information 3b an illustration of anisotropic margins in three dimensions is discussed. In the proposed framework, for every fraction a small percentage of the patients will be unable to reach the target dose, just as is the case for constant margins over the whole treatment. However, in the current approach, it is possible to increase the margins when a patient is on course to end with a dose below the target dose q. Therefore, in some cases, the intermediate target dose q_n becomes larger than 1.0. This occurs when the accumulated dose at some time during treatment becomes too low to get to the target q even when using infinite margins for the rest of the course. In a constant margin approach this problem does not occur by accepting 100%-p percentage of the patients failing to reach the dose q. To avoid unrealistically large margins in the adaptive approach we limit $q_n \leqslant 0.995$.

Because of this, it follows that the variable margin approach cannot guarantee to reach p percent of the population. For a fair comparison, we introduce p_{opt} in equation (3) and run the simulation experiments listed below with different p_{opt} such that for each experiment we arrive close to $p = 90\%$. The optimal interim population percentage p_{opt} was obtained by performing the simulations multiple times using different values in steps of 0.5%.

3. Simulations

In order to analyse the consequences of the adaptive margin approach we investigate the adaptive margin under similar assumptions as the van Herk recipe for margins. We assume a spherical CTV with radius R and a perfectly conformal dose distribution described by a gaussian convolution penumbra with width $\sigma_p = 3.2$ mm. Systematic and random errors are described by a three-dimensional normal distribution with widths Σ and σ respectively. We elaborate on the clinical relevance of this approach in the discussion.

For the accumulated dose to the CTV we limit our calculations to the edge of the CTV only, since that is where the minimum dose occurs in the limit of small errors compared to the size of the CTV. We discretise the surface of the CTV with 500 points using a Fibonacci sphere that almost equidistantly samples the sphere, for details we refer to the supplementary information, section 2. The systematic and random errors were sampled from a random number generator (Numpy v1.19.2, Python v3.8.5) with 3D normal distribution with widths Σ and σ. For all simulations we used a population size of 10 000 patients.

Before the adaptive margin simulations could be performed the margin function $M(N, q, p)$ had to be obtained. Numerous approximations to $M(N, q, p)$ have appeared in the literature (De Boer and Heijmen 2001, Gordon and Siebers 2007, Herschtal *et al* 2012), but we chose to obtain $M(N, q, p)$ from simulations. To this end we accumulated the dose on the edge of the CTV with N fractions using constant margins. We performed these simulations for margins ranging from 0 to 20 mm in steps of 0.25 mm. The function $M(N, q, p)$ can then be obtained from the cumulative population histogram of the minimum dose to the CTV using a linear interpolation on the numerical inverse of the histograms.

Random and systematic translations were sampled to create 10 000 individual treatment histories per set of parameters. The treatments with classical constant, adaptive isotropic or anisotropic margins were now simulated in parallel over the same histories. In the experiments we considered 3, 5, 7, 10, 15 and 20 fraction adaptive-margin radiotherapy. We investigated two cases representative of the different treatments used in clinical practice. The two case studies were a CTV ($R = 15$ mm) with a homogenous dose distribution ($q = 0.95$) and a small CTV ($R = 5$ mm) with an inhomogeneous dose distribution ($q = 0.80$). The systematic and random errors used for the two case studies were $\Sigma = 0, 1, 2$ mm and $\sigma = 1, 2, 3, 4$ mm.

For all experiments we stored for each simulated treatment the random and systematic motion, accumulated dose and margins per fraction. From these we extract descriptive statistics and create plots to investigate the possible individualised gains when using adaptive margins. For the anisotropic margins the per-fraction directional-averaged margins were stored. In the supplementary information (3c) we establish that these average margins can be used to estimate the resulting PTV volumes, also for the anisotropic case, via $Vol_{\mathrm{PTV}} = 4\pi/3 \times (R + m_{\mathrm{avg}})^3$.

4. Results

4.1. Margin simulations for finite fraction radiotherapy

In figure 2 the simulation results for $M(N, q, p)$ as a function of q for 2, 5 and 10 fractions with $p = 90\%$ are shown for the homogeneous case. As expected, necessary margins increase with a smaller number of fractions as do they with a larger standard deviation of the random and systematic errors. The necessary margins have an asymptote when q approaches 1, the dotted line in the figure indicates the limit we applied to avoid infinite margins for simulations with motions that could not be compensated in the remaining fractions by only increasing the margins. The other limit used in this work is that margins could not be negative. The correspondence of the function $M(N, q, p)$ with earlier work (De Boer and Heijmen 2001, Gordon and Siebers 2007) is provided in the supplementary information, figure S4, for reference.

4.2. Adaptive margins

As an illustration, we plotted for 10 treatments, out of the 10k simulations, the adaptive margin at each of the five fractions in figure 3 for both the anisotropic as isotropic margins to showcase the time evolution of the margins, for the same treatment histories. On average the margins decrease with time for both approaches reflecting that for most patients the motions are far below the used margins. For one treatment history, the grey hexagon, the adaptive isotropic margins are larger than the constant margins in the last fraction. For the anisotropic adaptive margins the directional-averaged margins are still lower, by enlarging the margins locally as indicated by the bars. This clearly indicates the benefit of anisotropic over isotropic adaptive margins to account for the observed motion pattern. For an overview of the evolution of the margins for the whole population we refer to the supplementary information, figures S7 and S8.

In figure 4(a) the vector length of the average motion over the course of treatment is plotted versus the treatment-averaged margins. On average a larger nett motion over the course of treatment results in larger

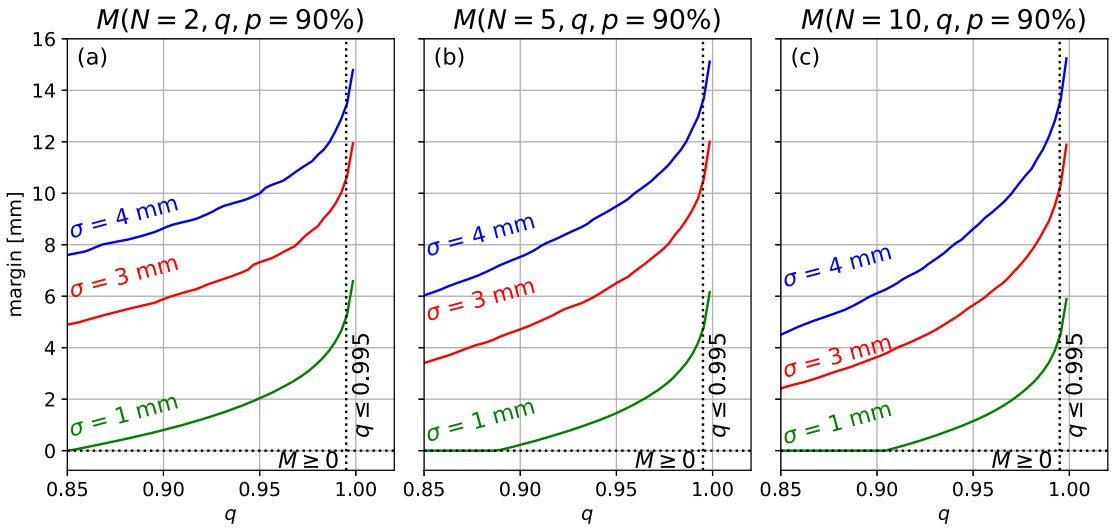

Figure 2. The margin function $M(N, q, p)$ as obtained from simulations for $N = 2$(a), 5(b) and 10(c) fractions as function of the target dose q for $\Sigma = 1$ mm and $\sigma = 1, 3, 4$ mm (green, red, blue) for the homogeneous dose distribution. Dotted lines represent the limits to the function as used in the adaptive margin analysis $M > 0; M < M(N, q = 0.995, p = 90\%)$.

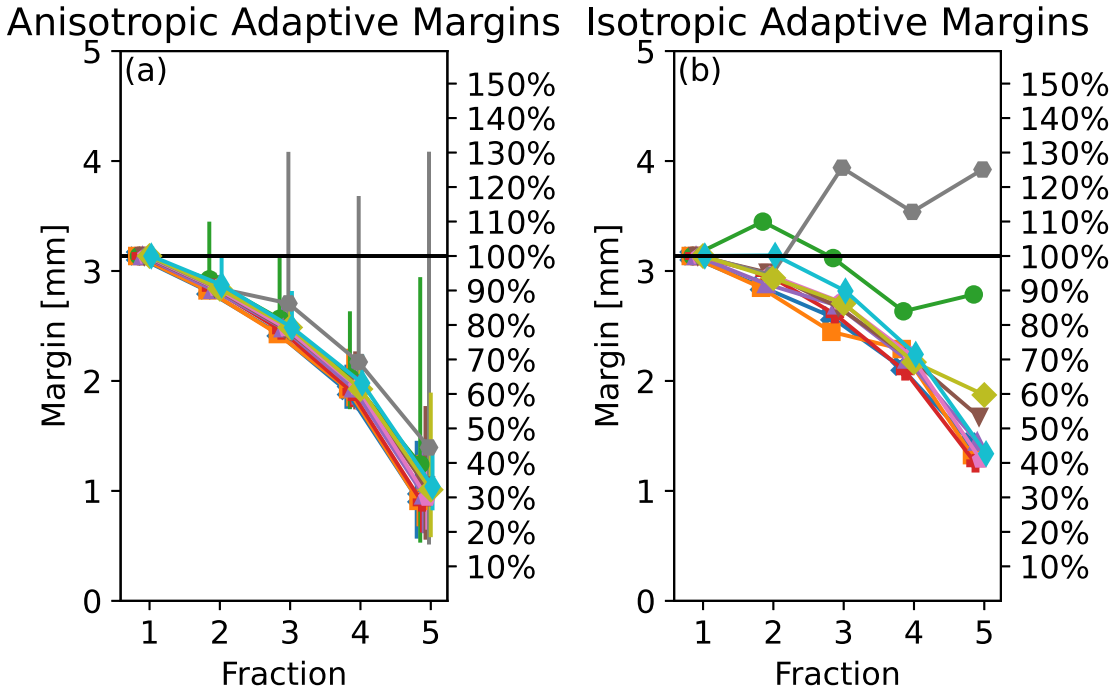

Figure 3. Time evolution of the adaptive margin strategies over a treatment of 5 fractions for 10 patients using anisotropic (a) and isotropic (b) adaptive margins, each line represents the margin over time for simulated individual treatments. For the anisotropic adaptive margins the directional-average margin is depicted. The corresponding necessary classical constant margin $m_c = 3.2$ mm is indicated with the horizontal line. Random and systematic errors were sampled using both σ and Σ of 1 mm. The sampled motion patterns were the same for the two adaptive margin strategies.

adaptive margins, with a larger spread for the isotropic margins. In figure 4(b) the relation between the accumulated CTV D_{min} and the treatment-averaged margin is shown color-coded for the total nett motion. From the figure it is clear that the treatment-averaged margins are reduced for the vast majority of patients in the anisotropic case and the majority for the isotropic case, also summarized in the histogram in figure 4(c). The trend of the figure indicates that patients with larger motions receive larger margins improving coverage for this group but, due to the construction of the recipe, still not enough for 10% of the population. But for the group of patients that show less than average motion, large margin reductions can be observed, as expected.

From figure 4(d) it can be seen that both the isotropic as anisotropic adaptive margins result in approximately the same distribution of CTV D_{min}. The adaptive approaches intersect the constant margin

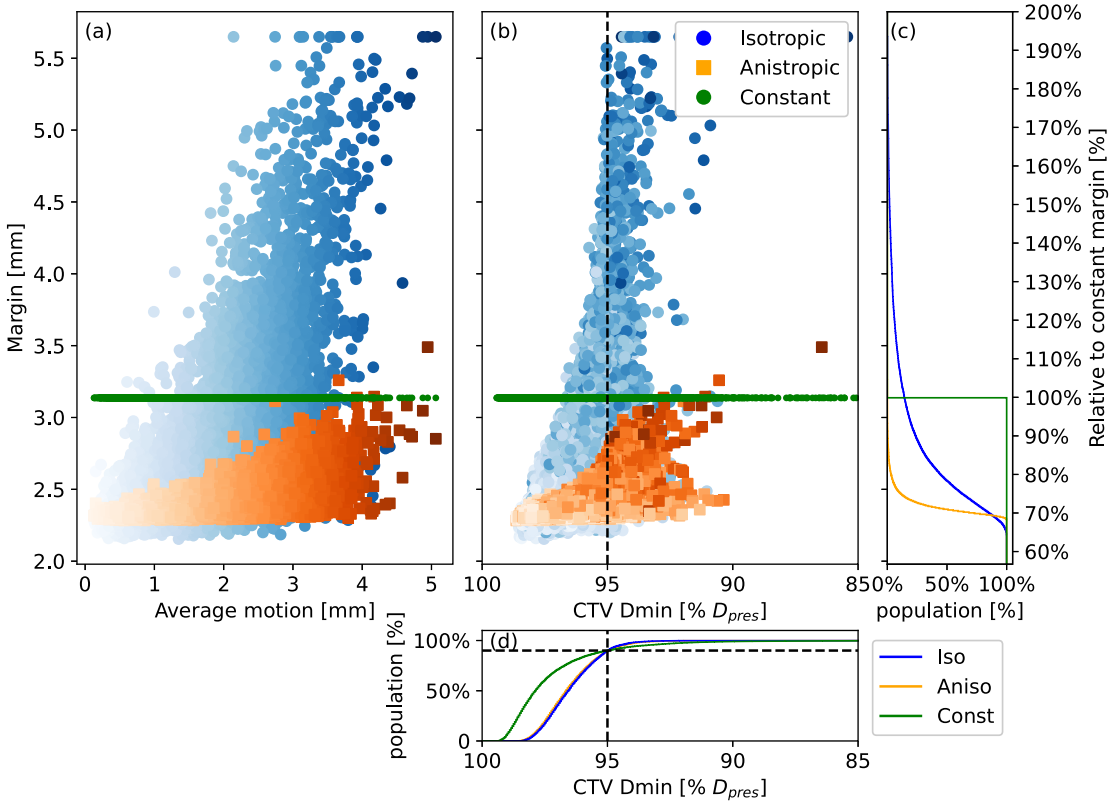

Figure 4. (a) Treatment-averaged margins after 5 fraction radiotherapy for (an)isotropic and constant margins versus vector length of average motion with σ and Σ of 1 mm in absolute margins or relative to the constant margins. The classical constant margin for this choice of parameters is given by $m_c = 3.2$ mm. (b) Margins versus minimum dose to the CTV at the end of treatment, hue-coded by average motion as in (a). The dots at the top of figures (a), (b) show the maximally allowed margins from the limit $q = 0.995$. In (c), (d) histograms along the y and x-axes are shown. In (d) the histograms for the isotropic and anisotropic adaptive margins overlap.

approach in the prescription point, what the methodology aimed for. The population difference in CTV $D_{\min}$ lies in the lower minimum CTV dose above the prescription dose and a higher minimum dose for the patients receiving a dose below the prescribed dose level. For these parameters the mean CTV $D_{\min}$ dose for this 10% of the population is 94.5% versus 92% when comparing the adaptive margins to the constant margins. Thus the individualised adaptive margins make the spread in CTV $D_{\min}$ smaller. These results were for a particular set of the parameters, but the general outline of this figure was consistent over all simulations and experiments.

Figures 5 and 6 summarize the main results for the treatment-averaged margins for the homogenous and inhomogeneous situation respectively. The boxplot indicates population mean, 25%–75% and 10%–90% of the population. In all situations the anisotropic adaptive margins were superior to isotropic adaptive margins, allowing for a larger population mean treatment-averaged margin reduction. For the homogenous case the population mean average margins over the whole treatment were in the range 75%–100% and 65%–95% of the constant margins for isotropic and anisotropic adaptive margins respectively. For the inhomogeneous case these numbers were 70%–80% and 55%–70%. The largest relative gain of the adaptive margins was for the longer treatments, but with most of the possible gain already achieved for courses consisting of five fractions. Furthermore, the adaptive margins also worked better for smaller random errors. The main difference between isotropic and anisotropic margins is clear, isotropic margins lead to a larger spread over the population, resulting for some of the patients in larger average margins compared to the constant margins and while others benefit more substantially, reflecting the differences in motion. In these figures we plotted the relative gains in margins. When comparing the results between different values of the systematic errors the largest *relative* gain was obtained for $\sum = 1$ mm. Since both the constant as the adaptive margins change significant with the systematic errors we cannot give a detailed explanation for this effect. We did so because different numbers of fractions result in different necessary constant margins. Conversion to absolute values can be done from the data listed in the supplementary information, section 3d. As described, in the simulations the parameter p_{opt} was used to arrive at $89\% < p < 91\%$. The percentage of the population satisfying CTV $D_{\min} \geqslant q$ at the end of all the simulated adaptive margins treatment was 90% in the range 88.8%–91.8% allowing for a fair comparison of the necessary margins. The used p_{opt} ranged between 80% and 96% in the anisotropic adaptive margins and from 50%–95% in the isotropic case. For all values see the tables in the supplementary information, tables S2, S5.

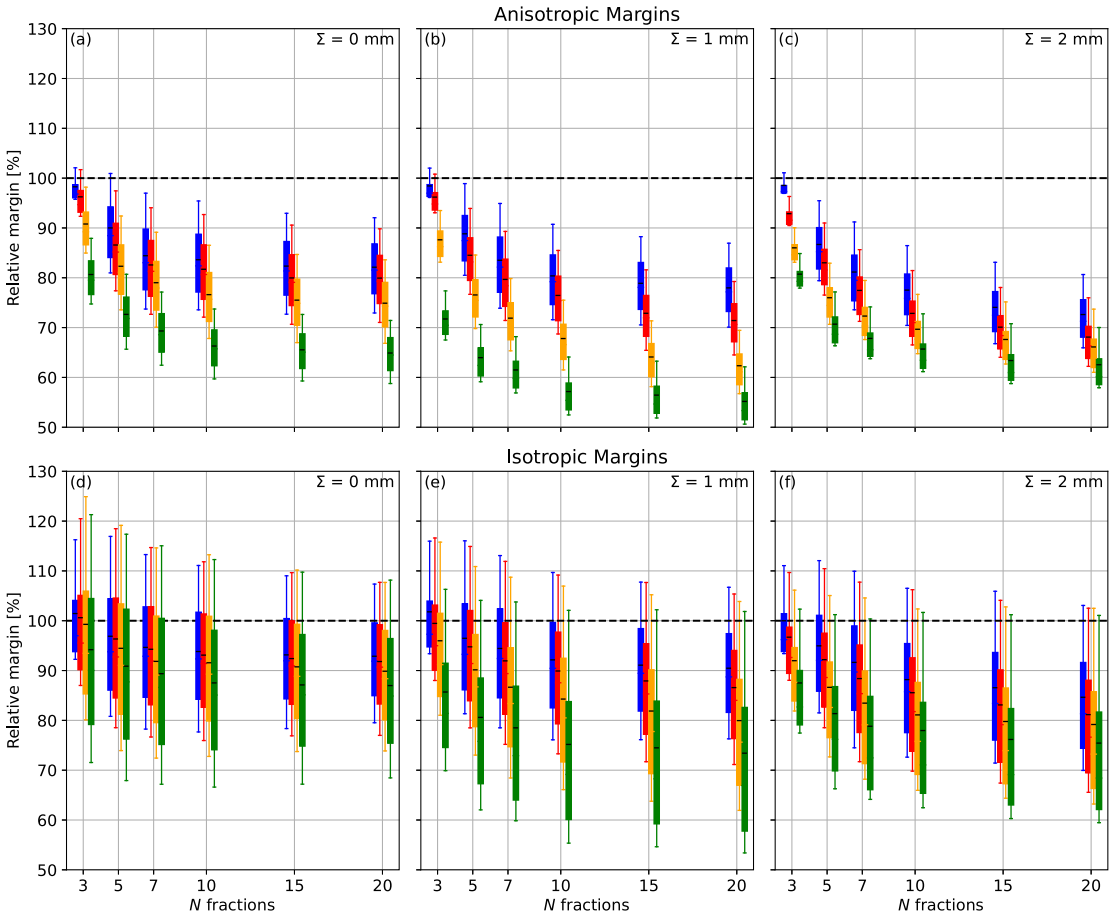

Figure 5. Boxplots of anisotropic (top row) and isotropic (bottom row) margins for the homogeneous dose distribution for all values of σ and $\sum$ for treatments of 3, 5, 7, 10, 15 and 20 fractions in length. All margins are given relative to constant margins m_c needed for the parameters and number of fractions. Boxes indicate interquartile range and mean treatment-averaged margins, whiskers indicate 10%–90% percentiles.

5. Discussion

In this work isotropic and anisotropic adaptive margins for online adaptive radiotherapy were considered, for a range of parameters. We demonstrated that the population mean of the average margins over the course of a radiation treatment can be reduced when margins are updated using the information gained about the individual patient and her or his treatment. The possible margin reduction was largest for inhomogeneously prescribed dose to the target. This can be understood from the fact that random motion is more easily compensated when the maximum dose in the target far exceeds the required minimum dose to the target. The anisotropic margins could be reduced to around 65% of the constant margins for the inhomogeneously prescribed dose. The resulting benefit in millimetres would only be 1–2 mm, as the margins necessary in this case are already small. This is partly due to the small systematic errors and random errors we used in these simulations which already led to relatively small treatment margins, one could say that improvements to online adaptive treatment planning are hard to make clinical relevant due to the small margins that are already possible, on the other hand, for certain groups, or individual patients on might try to use this laborious approach to get to the edge of what is possible. In this work we show how much can possibly be gained from adaptive margin strategies.

In this work we also simulated inhomogeneous dose distributions for longer treatment series (>7 fractions), currently such inhomogeneity is never used clinically for longer series, but to facilitate the comparison between the two methodologies we calculated the results for the same fractionation schemes.

We understand these modest gains from the following argument. The adaptive margins approach takes into account information about the individual treatment. In a way, we are updating our margins from a population-based estimate towards an individualised estimate as the treatment progresses. It is known that the estimation of treatment specific standard deviations from a limited number of samples only slowly converges $\sim n^{-1/2}$. The inclusion of a Bayesian prior improves the result but only slightly (Herschtal *et al* 2015). In other words: with a limited number of fractions, we have too little information to rule out a relatively large outlier in one of the next

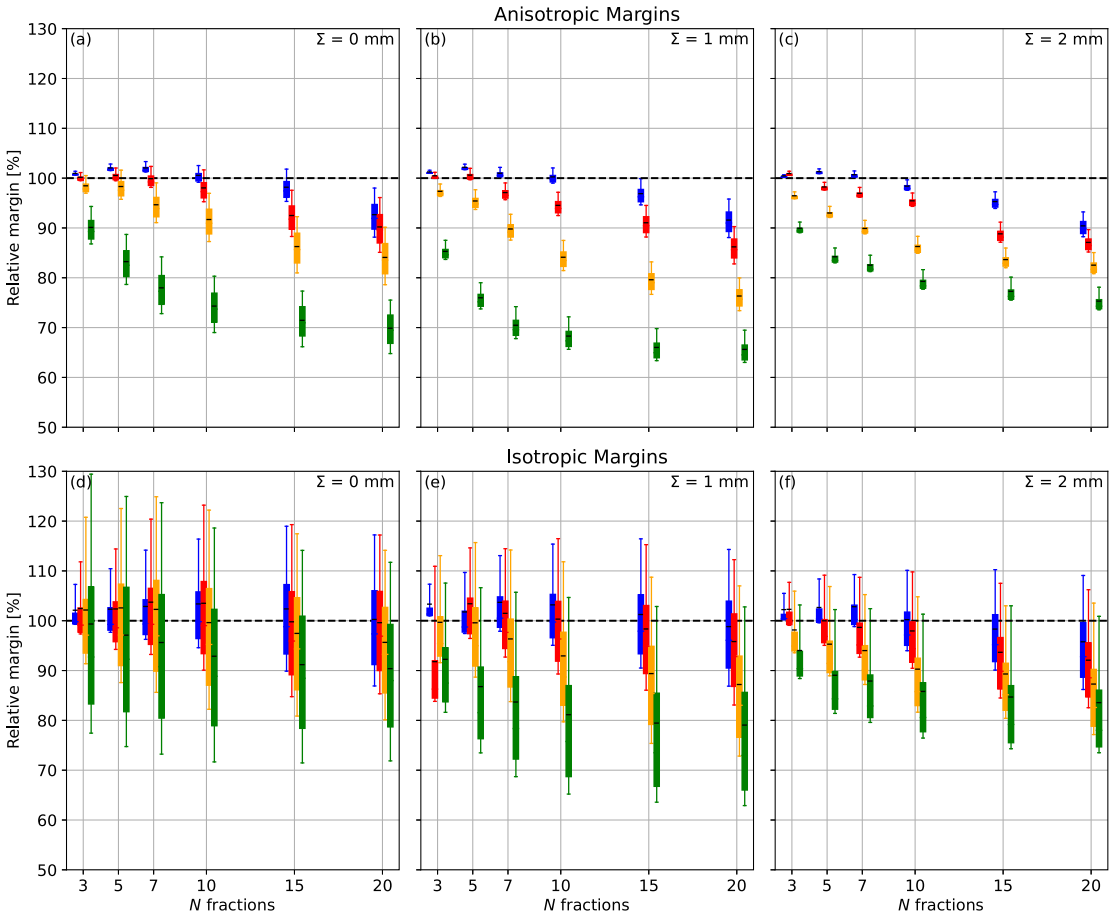

Figure 6. Boxplots of anisotropic (top row) and isotropic (bottom row) margins for the inhomogeneous dose distribution for all values of σ and $\sum$ for treatments of 3, 5, 7, 10, 15 and 20 fractions in length. All margins are given relative to constant margins m_c. Boxes indicate interquartile range and mean treatment-averaged margins, whiskers indicate 10%–90% percentiles.

fractions, which might dominate the required margin. Therefore, we cannot substantially decrease the margin based on the fractions given, especially so in extreme hypofractionated therapies. The main advantage for adaptive margins lies in the correction in the margin for the (effective) systematic motion that repeats itself from fraction-to-fraction, and becomes more relevant in longer treatment series.

Our methodology to obtain adaptive margins is independent of the margin recipe used. However in order to calculate the effects of adaptive margins we employed the same framework as those used for calculation of margins in the van Herk recipe, with all its simplifications as stated in the introduction. Our simulation results for *M(N, q, p)* were in line with previous works (Van Herk *et al* 2000, De Boer and Heijmen 2001, Gordon and Siebers 2007, Herschtal *et al* 2012). The simplifications of this approach and corresponding limitations are discussed often in literature, however, it still is the most used approach to estimate the necessary radiotherapy treatment margins. We think our results should be interpreted with the same caution as the classical margin recipes should be, and think that is has clinical relevance just as the classical margin recipe. While the results presented are explicitly based on the idealized situation of the van Herk margin recipe, our strategy for margin adaptation is generalizable to any margin approach. One could for example consider combining our approach with robust planning algorithms for proton therapy(Unkelbach and Paganetti 2018). In this case robust treatment plan would be generated for each fraction in such a way that, given the already delivered dose, the target will be adequately covered with suitable probability.

We needed to introduce the p_{opt} parameter to facilitate a fair comparison between the adaptive and constant margins. This necessity stemmed from keeping the margins positive and the restriction of $q_n \leqslant 0.995$ to avoid margins that became unrealistically large. For the parameters with small systematic and random errors, some of the patients would need negative margins to aim for a population coverage of 90%. Since these were not allowed the interim p_{opt} needed to be increased. Similarly, limiting the margins from becoming unrealistically large leads to a lower p_{opt}.

In order to limit the amount of simulations choices were made for the parameters used. For the prescription we only considered $p = 90\%$ and $q = 0.95$ and $q = 0.8$ in line with our institution prescriptions. Other choices

would lead to slightly different results. The choices for the penumbra and the cases used in this paper were made to be comparable to previous literature. The systematic and random standard deviations were chosen such that the resulting margins were within the range of margins reported for online adaptive radiotherapy 2–7 mm (de Bohoudi *et al* 2017, Winkel *et al* 2019, Muinck Keizer *et al* 2020, Intven *et al* 2021, Kensen *et al* 2022). As a consequence, the resulting considered systematic errors in the range 0–2 mm were relatively small. This may be partly due to the fact that in online adaptive radiotherapy parts of the systematic errors should be considered random due to the daily update of contours and plans. Given that the adaptive margins are better at reducing margins caused by systematic errors we expect the methodology work better for larger systematic errors.

In this work we estimated the margin for the next fraction from the dose given thus far. The errors used throughout this paper thus represent the *known* errors. However, *unknown* errors are not taken into account. These could be associated with incorrect modelling of the dose in the planning system, registration errors involved in the dose accumulation, or differences between the beam isocentre and imaging isocentre and of course delineation uncertainty(Burbach *et al* 2016). A systematic understanding how known and unknown random and systematic errors influence online adaptive radiotherapy remains to be understood in general and taking them into account here was outside the scope of the current work.

In the simulations only translations of the CTV were considered for the evaluation of the accumulated dose and resulting margins. In clinical reality intrafraction motion is much more complex. These motions were not explicitly taken into account in this work. However if a proper way for intrafraction dose accumulation would exist, the methodology to obtain the margin for the next fraction would still be valid. Intrafraction motion would result in an effective blurring of the dose distribution. This is why in a margin approach considering an infinite number of fractions, intrafraction motion can be added to the random error. In our model with a finite number of fractions, this is not exactly true, but could be considered a first approximation.

We used the running average margins per patient as proxy for an estimation of the therapeutic gain since this geometric values represent the most straightforward and interpretable choice to make. However, the clinical effect of adaptive margins on the dose to nearby organs at risk depends on their radiobiological response. For parallel organs at risk the risk depends on the total irradiated volume which scales with the third power of the margin making even small margin reductions worthwhile. Our current analysis focusses on potential margin decrease in an idealized situation. The dosimetric or clinical impact of this in clinical practice should be carefully studied on a treatment site specific basis.

The two models for adaptive margins considered here are idealized recipes and probably not feasible in clinical practice in the near future. This is due to the fact that dose accumulation over the course of treatment is not readily available and, even when it would be, the uncertainties involved in the (deformable) registration and possible motion during dose delivery would probably introduce additional complications for the estimated minimum dose given thus far. In addition to these difficulties, the generation of a different margin for every solid angle around the (non-spherical) CTV is not clinically available. Application of the anisotropic margin to six main directions ($\pm x$, $\pm y$, $\pm z$) would lead to ambiguities in the definition the margin for each simulation point and modelling of the dose distribution, Therefor we have chosen to present the most idealised adaptive margin strategy in this work to estimate its maximum potential gain.

In this work only perfectly conformal and homogeneous (adapted) treatment plans were assumed in the modelling. In clinical practice local hotspots or digressions from conformity are a reality. Although the adaptive margins derived from the accumulated dose will correct some of these effects, coldspots in the CTV cannot be accounted for, because the current work only considered adjusting treatment margins without changing locally the dose distribution within the PTV. In this work, we only adapted the treatment margin. However, further improvement of our approach might be achievable when adaptive margins are combined with locally increasing or decreasing the dose relative to what is been given. How to do such adaptive dose painting is outside the scope of this work.

6. Conclusion

In this work adaptive radiotherapy margins were introduced for online adaptive radiotherapy. When dose accumulation becomes readily available, the proposed methodology for adaptive margins becomes feasible. The methodology leads to a modest decrease in treatment margins for the population mean, ranging from 65% to 95% (1–2 mm) of the corresponding classical margins. For individual patients the results become more pronounced, since patients that happen to have average target motion below the population average will receive substantially smaller margins. On the other hand, patients with larger than average motion will require an increased margin. Moreover, for the 10% of patients that would not reach the desired coverage due to the definition of the margin recipe, the minimum dose to the target is increased by using adaptive margins. As such,

the approach leads to slightly improved radiotherapy on the group level, but might have substantial benefits for the individual patient, be it in smaller margins, or better target coverage.

ORCID iDs

Erik van der Bijl https://orcid.org/0000-0001-7663-4390
Jan-Jakob Sonke https://orcid.org/0000-0001-5155-5274
Tomas Janssen https://orcid.org/0000-0003-2807-8670

References

Acharya S *et al* 2016 Online magnetic resonance image guided adaptive radiation therapy: first clinical applications *Int. J. Radiat. Oncol., Biol., Phys.* **94** 394–403

Ahmad R, Bondar L, Voet P, Mens J-W, Quint S, Dhawtal G, Heijmen B, Hoogeman M and Hoogeman M 2013 A margin-of-the-day online adaptive intensity-modulated radiotherapy strategy for cervical cancer provides superior treatment accuracy compared to clinically recommended margins: a dosimetric evaluation *Acta Oncol.* **52** 1430–6

Bel A, Van Herk M and Lebesque J V 1996 Target margins for random geometrical treatment uncertainties in conformal radiotherapy *Med. Phys.* **23** 1537–45

Boer H C J D and Heijmen B J M 2001 A protocol for the reduction of systematic patient setup errors with minimal portal imaging workload *Int. J. Radiat. Oncol., Biol., Phys.* **50** 1350–65

Bohoudi O, Bruynzeel A M E, Senan S, Cuijpers J P, Slotman B J, Lagerwaard F J and Palacios M A 2017 Fast and robust online adaptive planning in stereotactic MR-guided adaptive radiation therapy (SMART) for pancreatic cancer *Radiother. Oncol.* **125** 439–44

Burbach J P M, Kleijnen J P J, Reerink O, Seravalli E, Philippens M E P, Schakel T, Van Asselen B, Raaymakers B W, Van Vulpen M and Intven M 2016 Inter-observer agreement of MRI-based tumor delineation for preoperative radiotherapy boost in locally advanced rectal cancer *Radiother. Oncol.* **118** 399–407

Collins S D and Leech M M 2018 A review of plan library approaches in adaptive radiotherapy of bladder cancer *Acta Oncol.* **57** 566–73

Gordon J J and Siebers J V 2007 Convolution method and CTV-to-PTV margins for finite fractions and small systematic errors *Phys. Med. Biol.* **52** 1967-–90

Herk M V, Remeijer P, Rasch C and Lebesque. J V 2000 The probability of correct target dosage: dose-population histograms for deriving treatment margins in radiotherapy *Int. J. Radiat. Oncol., Biol., Phys.* **47** 1121–35

Herk M V 2004 Errors and margins in radiotherapy *Semin. Radiat. Oncol.* **14** 52–64

Herschtal A *et al* 2015 Calculating radiotherapy margins based on bayesian modelling of patient specific random errors *Phys. Med. Biol.* **60** 1793–805

Herschtal A, Foroudi F, Silva L, Gill S and Kron T 2012 Calculating geometrical margins for hypofractionated radiotherapy *Phys. Med. Biol.* **58** 319–33

Intven M P W, de Mol van Otterloo S R, Mook S, Doornaert P A H, de Groot-van Breugel E N, Sikkes G G, Willemsen-Bosman M E, van Zijp H M and Tijssen R H N 2021 Online adaptive MR-guided radiotherapy for rectal cancer; feasibility of the workflow on a 1.5T MR-linac: clinical implementation and initial experience *Radiother. Oncol.* **154** 172–8

Jong R D, Crama K F, Visser J, Van Wieringen N, Wiersma J, Geijsen E D and Bel A 2020 Online adaptive radiotherapy compared to plan selection for rectal cancer: quantifying the benefit *Radiat. Oncol.* **15** 162–71

Kensen C M, Janssen T M, Betgen A, Wiersema L, Peters F P, Remeijer P, Marijnen C A M and van der Heide U A 2022 Effect of intrafraction adaptation on PTV Margins for MRI guided online adaptive radiotherapy for rectal cancer *Radiat. Oncol.* **17** 110–19

Muinck Keizer D M D, Kerkmeijer L G W, Willigenburg T, van Lier A L H M W, den Hartogh M D, van der Voort van Zyp J R N, de Groot-van Breugel E N, Raaymakers B W, Lagendijk J J W and de Boer J C J 2020 Prostate intrafraction motion during the preparation and delivery of MR-guided radiotherapy sessions on a 1.5T MR-linac *Radiother. Oncol.* **151** 88–94

Mutic S and Dempsey J F 2014 The ViewRay system: magnetic resonance–guided and controlled radiotherapy *Semin. Radiat. Oncol.* **24** 196–9

Peulen H, Belderbos J, Rossi M and Sonke J J 2014 Mid-ventilation based PTV margins in stereotactic body radiotherapy (SBRT): a clinical evaluation *Radiother. Oncol.* **110** 511–6

Raaymakers B W *et al* 2017 First patients treated with a 1.5 T MRI-linac: clinical proof of concept of a high-precision, high-field MRI guided radiotherapy treatment *Phys. Med. Biol.* **62** L41–50

Sibolt P, Andersson L M, Calmels L, Sjöström D, Bjelkengren U, Geertsen P and Behrens C F 2021 Clinical implementation of artificial intelligence-driven cone-beam computed tomography-guided online adaptive radiotherapy in the pelvic region *Phys. Imaging Radiat. Oncol.* **17** 1–7

Unkelbach J and Paganetti H 2018 Robust proton treatment planning: physical and biological optimization *Semin. Radiat. Oncol.* **28** 88–96

Winkel D *et al* 2019 Adaptive radiotherapy: the elekta unity MR-Linac concept *Clin. Transl. Radiat. Oncol.* **18** 54

Winkel D, Bol G H, Werensteijn-Honingh A M, Kiekebosch I H, van Asselen B, Intven M P W, Eppinga W S C, Raaymakers B W, Jürgenliemk-Schulz I M and Kroon P S 2019 Evaluation of plan adaptation strategies for stereotactic radiotherapy of lymph node oligometastases using online magnetic resonance image guidance *Phys. Imaging Radiat. Oncol.* **9** 58–64